Tissue-Engineered Tendon Constructs for Rotator Cuff Repair in Sheep[1]

Stoyna S. Novakova[1], Vasudevan D. Mahalingam[1], Shelby E. Florida[1], Christopher L. Mendias PhD[1,2], Answorth Allen MD[2,6], Ellen M. Arruda PhD[3,4,5], Asheesh Bedi MD[2] and Lisa M. Larkin PhD[1,4]

[1]Departments of Molecular and Integrative Physiology, The University of Michigan, Ann Arbor, MI 48109-2200

[2]Departments ofOrthopaedic Surgery, The University of Michigan, Ann Arbor, MI 48109-2200

[3]Departments ofMechanical Engineering, The University of Michigan, Ann Arbor, MI 48109-2200

[4]Departments ofBiomedical Engineering, The University of Michigan, Ann Arbor, MI 48109-2200

[5]Departments of Macromolecular Science and Engineering, The University of Michigan, Ann Arbor, MI 48109-2200.

[6]Hospital for Special Surgery, New York, NY

Corresponding Author: Lisa Larkin PhD
Professor
Molecular and Integrative Physiology
Biomedical Engineering
University of Michigan
Biomedical Science Research Building (BSRB)
109 Zina Pitcher Place, Room #2025
48109-2200
Phone: (734) 936-8181

[1] This is the author manuscript accepted for publication and has undergone full peer review but has not been through the copyediting, typesetting, pagination and proofreading process, which may lead to differences between this version and the Version of Record. Please cite this article as doi:10.1002/jor.23642

Fax: (734) 615-3292
e-mail: llarkin@umich.edu

Running Title: Engineered Tendon Rotator Cuff Repair

Contributions: S.S.N., V.D.M., E.M.A., A.B., L.L.M. contributed to research design.
S.S.N., V.D.M., S.E.F., C.L.M. contributed to data acquisition.
S.S.N., V.D.M., E.M.A., A.B., L.L.M. analyzed and interpreted the data.
S.S.N., V.D.M., S.E.F., C.L.M., A.A, E.M.A., A.B., L.L.M contributed to critically revising the paper and approving the submitted version.

ABSTRACT

Current rotator cuff repair commonly involves the use of single or double row suture techniques, and despite successful outcomes, failure rates continue to range from 20-95%. Failure to regenerate native biomechanical properties at the enthesis is thought to contribute to failure rates. Thus, the need for technologies that improve structural healing of the enthesis after rotator cuff repair is imperative. To address this issue, our lab has previously demonstrated enthesis regeneration using a tissue-engineered graft approach in a sheep anterior cruciate ligament (ACL) repair model. We hypothesized that our tissue-engineered graft designed for ACL repair also will be effective in rotator cuff repair. The goal of this study was to test the efficacy of our Engineered Tissue Graft for Rotator Cuff (ETG-RC) in a rotator cuff tear model in sheep and compare this novel graft technology to the commonly used double row suture repair technique. Following a 6-month recovery, the grafted and contralateral shoulders were removed, imaged using x-ray, and tested biomechanically. Additionally, the infraspinatus muscle, myotendinous junction, enthesis, and humeral head were preserved for histological analysis of muscle, tendon, and enthesis structure. Our results showed that our ETC-RCs reached 31% of the native tendon tangent modulus, which was a modest, non-significant, 11% increase over that of the suture-only repairs. However, the histological analysis showed the regeneration of a native–like enthesis in the ETG-RC-repaired animals. This advanced structural healing may improve over longer times and may diminish recurrence rates of rotator cuff tears and lead to better clinical outcomes.

Keywords: tendon repair, tissue engineering, scaffold-free, sheep, rotator cuff

INTRODUCTION

Rotator cuff (RC) tears are a major orthopedic challenge in the United States with over 200,000 repair procedures performed annually resulting in approximately $474 million dollars in

health care costs [1]. Furthermore, it is estimated that tendon tears affect 21 - 27% of people over the age of 60 with the prevalence increasing with age [2-3]. Currently, the primary method for rotator cuff repair utilizes a single or double row suture technique to secure the ruptured tendon to its attachment interface (enthesis) on the bone. However, despite advancements in repair techniques, repairs fail 20-95% of the time, with the greatest incidence of failure in repairs of full-thickness tears [4-5]. Due to the complex anatomy of the shoulder joint, multiple factors may contribute to these observed failure rates, including the severity of the tear, poor vascularization of the tendon, fatty infiltration, increased scarring leading to decreased range of motion, and muscle atrophy [6-7]. Most importantly, high failure rates are likely due to the inability of current treatment techniques to regenerate an enthesis, the native tendon to bone interface, and instead form a weaker, less organized fibrovascular scar tissue that is prone to failure. An enthesis, or tendon to bone attachment site, has four transitional zones that create a structurally continuous gradient of tissue from tendon, through unmineralized fibrocartilage, and mineralized fibrocartilage, and then to bone [8-10]. The zonal composition of an enthesis has been well described in the literature [9-13]. The mechanical properties of tendon and bone differ significantly, with bone having a modulus of 20 GPa and tendon with a modulus of approximately 200 MPa. The orientation of the collagen fiber alignment within the enthesis, combined with stratification of the enthesis materials, has been shown to affect the maximum values of stresses and strains in the enthesis [14]. Therefore, it is thought that the physiological enthesis shape and constitution minimize the stress in the region.

Thus, it is thought that the regeneration of a native enthesis is critical to improving clinical outcomes for patients with RC tears. As such, various tissue-engineering strategies are being developed to improve surgical outcomes and promote tendon healing, especially at the

enthesis. Current techniques, however, focus on the development of biological or synthetic scaffold devices to reinforce the mechanical strength of the tendon-to-bone connection. During 2010 in the United States alone, nearly 30,000 rotator cuff repairs were mechanically reinforced with biological or synthetic patches [15]. However, these current patch technologies do not promote enthesis regeneration. It is likely that enthesis regeneration following the use of these patch repair strategies is limited by the variability in the degradation rates of scaffold materials, which do not match the rate of new matrix production at the regenerating tendon to bone interface [16]. Moreover, the use of stiff scaffolding material designed for initial strength may shield the host cells from mechanical signals required for optimal tissue remodeling during regeneration [17-18]. Thus, there is a demand for alternative technologies for repair of tendon injuries.

Previous work from our lab showed successful use of scaffold-less multiphasic bone-ligament-bone (BLB) grafts for the repair of an anterior cruciate ligament (ACL) injury. Used as an ACL replacement graft, these BLB constructs regenerated a new ACL with the structural and biomechanical properties of a native ACL including a native-like enthesis [19-21]. These favorable results prompted our laboratory to apply this same technology in a rotator cuff repair model in sheep.

Thus, the purpose of this study was to compare our scaffold-less tissue-engineered tendon graft designed for rotator cuff repair (ETG-RC) to suture-only techniques in the repair of the infraspinatus tendon in a sheep model. Our goal was to evaluate enthesis regeneration between the two repair groups through histomorphological and biomechanical measures. We hypothesized that the utilization of our ETG-RC as an underlay that is interposed between the

infraspinatus tendon and bone would improve enthesis regeneration and collagen organization over the commonly used double suture-only technique.

MATERIALS AND METHODS

Species Justification & Animal Care

The sheep is a suitable model because the rotator cuff tendons are similar in size to that of humans, which from a translational standpoint allows for similar suturing techniques to improve repairs. Female Black Suffolk sheep (n=23) (Ovis aries; age, 10 to 12 mo; weight, 55 to 105 kg) were determined to be healthy by physical examination by a veterinarian at the University of Michigan's Unit for Laboratory Animal Medicine (ULAM). All sheep were housed in groups within approved large animal facilities for the duration of the study and randomly assigned to 1 of 2 experimental groups: ETG-RC repair or suture-only (SO) repair. The left shoulder was designated as the experimental RC tear and repair with the unoperated contralateral right shoulder serving as control for all animals in the study. BMSCs harvested from an adult male Black Suffolk sheep were used to fabricate our constructs. The fabricated ETG-RCs were then implanted into the female recipients, as described below. All animals were acclimated to the ULAM husbandry facilities at the University of Michigan for at least one week prior to any

procedure. Sheep were given access to food and water *ad libitum*. All animal care and animal surgeries were performed in accordance with The Guide for the Care and Use of Laboratory Animals [24] and the experimental protocol was approved by the University Committee for the Use and Care of Animals.

Media Preparation

All solutions and media were prepared and stored at 4°C and were warmed to 37°C prior to use (Supplementary Methods).

Isolation and Expansion of BMSCs

Using previously described methods [20-21], bone marrow stromal cells were harvested from an iliac crest marrow aspiration of an adult male sheep using a Monoject Illinois needle (Sherwood Medical Company, St. Louis, Mo**)** (Supplementary Methods).

Fabrication of ETG-RCs

We fabricated ETG-RC constructs to span the enthesis as an underlay that is interposed between the infraspinatus tendon and bone (Figure 1): one end of the construct splayed out to anchor the tendon at multiple points, and the opposite end compacted to fit inside a bone tunnel drilled in to the humerus at the site of the enthesis (Supplementary Methods; Figure 2). Prior to surgical implantation, constructs were retrieved from the freezer and allowed to thaw in a 4°C fridge for a minimum of one hour.

In vitro ETG-RC characterization

To examine morphological characteristics of the *in vitro* ETG-RC, staining with hematoxylin and eosin (H&E), Picrosirius red, and elastin was performed (Supplementary Methods).

Surgical Techniques and Procedure

Prior to surgery, sheep were randomly divided into two different surgical repair groups and fasted for 12 h. A fentanyl patch (75 µg) was attached to their skin to provide pre-emptive analgesia. Xylazine (0.22 mg/kg IM; MWI, Boise, ID) and propofol (6 mg/kg IV, MWI, Boise, ID) were administered for induction of general anesthesia (Supplementary Methods). A 6 cm skin incision was made over the shoulder joint to expose the deltoid. The deltoid was then split along the tendinous division between the acromial and scapular heads to gain access to the underlying infraspinatus tendon. The insertion of the superficial head of the infraspinatus tendon was isolated, and the entire tendon was detached from its attachment on the tuberosity to simulate a RC tear. All tears were repaired immediately using either an ETG-RC repair (n=12), where ETG-RCs were implanted as an underlay that is interposed between the infraspinatus tendon and bone in combination with the double-row suture technique, or with a double-row suture technique only (n=11) (Supplementary Methods).

Explantation

After a six-month recovery, the animals were euthanized (Supplementary Methods). During necropsy, both shoulders were harvested by removing the humerus and scapula while keeping the rotator cuff intact. The surgical site was grossly examined and observations were recorded and digitally photographed. Radiographs were taken for the grafted and contralateral shoulders to assess the health of the bone, tendon, and the recovery of the bone tunnels. Shoulders were then further dissected to isolate the infraspinatus tendon with the humerus and scapula still attached for morphological, histological, and biomechanical analyses. Additionally, biopsies of the infraspinatus muscle, approximately 2 mm in diameter and 10 mm in length, were obtained and prepared for histological analysis and single muscle fiber contractility measurements.

Radiographs

A grading system was devised to assess the extent of mineralization of the infraspinatus tendon (Supplementary Methods). Statistical analysis of specimen brightness was performed using a Student's t-test with P value < 0.05 considered significant. Data are presented as mean ± standard error.

Muscle Histological Analysis

The infraspinatus muscle samples were frozen in Tissue-Tek ® O.C.T (Triangle Biomedical Sciences, Durham, NC) using isopentane (Fisher Chemical, Fair Lawn, NJ, USA) cooled with dry ice and stored at −80°C. Frozen muscles were cross-sectioned at a thickness of 12μm and prepared for immunohistochemistry (IHC) for fiber type analysis (Supplementary Methods). A minimum of five specimens for each repair group and respective contralateral shoulders were randomly selected and analyzed. Muscle fiber size and percentage of fibers containing different myosin heavy (MHC) isoforms (type I and type II) was evaluated within a randomly selected fascicle of the infraspinatus muscle. Fiber cross-sectional area (CSA) measurements for each cross-section were performed by outlining fibers using ImageJ software. Fiber counts, fiber type percentages, and CSAs are reported as mean ± standard deviation.

Single Muscle Fiber Contractility

At the single muscle fiber level, contractility was evaluated using methods previously described [25-26] (Supplementary Methods). Fast fibers (n=8) were tested from each specimen and the average value was used in statistical analyses.

Tendon Biomechanical Testing

Immediately after dissection, biomechanical testing was performed on the isolated infraspinatus tendons. The tendons were tested in uniaxial configuration by mounting the

humerus and scapula using custom-designed grips onto a material testing system (MTS 810 servo-hydraulic system) with a 25 kN load cell (Supplementary Methods). The modulus of elasticity was calculated by computing the slope of the stress-strain curve in the 0.075 – 0.090 strain range.

Histological Analysis of Enthesis

To examine the enthesis, each specimen was trisected along the long axis of the infraspinatus tendon and its humeral attachment site in the transversal plane into sections using a scalpel for the tendon and a diamond blade pathology saw for the humerus (EXAKT 312, Oklahoma City, OK, U.S.A). Digital images were taken of each specimen following sectioning to assess the repair of the enthesis between bone and tendon. The specimens were fixed in 10% neutral buffered formalin for 48 hours and decalcified in 10-20% EDTA. Samples were X-rayed weekly to determine successful decalcification. Once radiographs confirmed the absence of calcium deposits, the samples were processed using a standard processing schedule in an automated Histocore Arcadia System (Leica Biosystems Inc., Buffalo Grove, IL, USA) tissue processor and embedded in Paraplast paraffin wax (Sigma-Aldrich, St. Louis, MO, USA). 7-µm thick serial sections, containing the repaired tendon and greater tuberosity of the humerus, were cut and stained with picosirius red, Masson's trichrome, hematoxylin and eosin (H&E), and alizarin (Supplementary Methods). Prior to staining, paraffin-embedded sections were deparaffinized using xylene and rehydrated through decreasing grades of ethanol. Using an Olympus BX-51 light microscope, digital images of the stained slides were taken using a SPOT RT camera (Diagnostic Instruments, Sterling Heights, Michigan). Additionally, distal segments of the infraspinatus tendon were frozen in Tissue-Tek using dry ice cooled isopentane and stored at -80ºC until use. Tendons were cryosectioned at a thickness of 12 µm and stained.

Statistical Analysis

The biomechanical and histological outcomes of the two repair scenarios were compared using one-way ANOVA with Tukey's post hoc test with significance indicated by a $P < 0.05$. Radiographs were analyzed using a Student's t-test with significance indicated by a $P < 0.05$. Data are reported as mean ± standard deviation. Prism 7.0 software (GraphPad Software, La Jolla, CA. USA) was used to perform statistical analysis.

RESULTS

Gross Morphology of the Surgical Site

At the time of sacrifice, all animals appeared healthy and showed no signs of infection, pain, or failed repairs. Two sheep from the ETG-RC repair group were excluded from the study prior to the 6-month endpoint measures. One of the sheep died, unexpectedly, of a *C. perfringens* type A enterotoxemia. The other sheep was sacrificed at an earlier time point to evaluate the progress of the repair after 4 months. The regeneration of the tendon was less than optimal, so remaining sheep were allowed to recover for an additional 2 months. At the 6-month recovery time, gross evaluation of the infraspinatus tendon and humerus showed increased connective tissue in suture-only repaired shoulders compared to ETG-RC repaired shoulders (Figure 4 D-F). However, both repair techniques had more connective tissue compared to contralateral shoulders. The cross-sectional area of the infraspinatus tendon was measured and both repair techniques resulted in a tendon with a significantly greater ($P<0.001$) CSA than native (79.6 ± 32.60 mm^2). Although, the CSA of the tendons in the suture-only repairs (270.7 ± 127.1 mm^2) trended towards greater CSAs values ($P=0.1063$) than ETG-RC (198.0 ± 81.13 mm^2) repairs.

Radiograph Analysis of the Infraspinatus Tendon

Radiographs of the shoulder joint showed appropriate and consistent anchor placement with no significant degradation in either of the surgical groups (Figure 4 A-C). However, during the histological analysis of the infraspinatus tendon, mineralized regions within the tendon were discovered. Thus, the radiographic views of the shoulder were used to examine and quantify the extent of mineralization in the repaired infraspinatus tendons and compared to the contralateral control infraspinatus tendon (Figure 5 A-D). The mean grayscale values of the contralateral infraspinatus tendons in the ETG-RC and suture-only groups were not significantly different, 104 ± 6 and 104 ± 5, respectively. Analysis of the infraspinatus tendons in the ETG-RC group showed no mineralization and were not significantly different from their respective contralateral tendons having a mean grayscale value of 105 ± 6. However, the suture- only group had a significantly higher (P=0.0003) mineral content in the infraspinatus tendons than the respective contralateral shoulders (117 ± 6 grayscale units; Figure 5E).

Biomechanical Testing of Infraspinatus Tendon

Following 6 months of recovery, RC tears repaired with either ETG-RC or suture technique displayed no difference in tangent modulus between repair groups. However, both repair groups were significantly less stiff than contralateral shoulders (Figure 6). The mean modulus of the tendon-bone interface was as follows: contralateral (106 ± 24 MPa, n=20, P<0.0001 ETG-RC, P<0.0001 SO), ETG-RC repair (33± 16 MPa, n=10, P=0.34), and suture-only repair (21 ± 7 MPa, n=11, P=0.34).

Histomorphometric Analysis of the Enthesis and Infraspinatus Tendon

Picrosirius red staining was used to evaluate tissue collagen alignment at the enthesis interface. Collagen birefringence showed that contralateral and ETG shoulders had significantly greater collagen alignment compared to suture-only repaired shoulders. ETG-RC repaired

shoulders were not significantly different from contralateral shoulders (Figure 7 A-C). Contralateral shoulders had an average brightness value of 81±18 grayscale units. ETG-RC repairs had a mean brightness grayscale value of 75 ±12, while suture-only repairs had a value of 47 ± 9 grayscale units (Figure 7D). The increase in brightness intensity of ETG-RC repairs suggests an increase in remodeling of the collagen fiber architecture to a properly organized collagen fiber framework and resembles native enthesis. In contrast, the suture-only repair appears to be comprised of disorganized scar tissue at the interface.

The amount of proteoglycan content was evaluated at the enthesis by determining the area of metachromasia of trichrome stained sections. Overall, no significant difference in area of fibrocartilage formation was observed in ETG-RC or suture-only repairs, although suture-only repairs trended towards a higher percent of metachromasia formation (Figure 7 E-G). The percent area of metachromasia, or fibrocartilage, at the enthesis for each group was as follows: contralateral shoulders (40 ± 19), ETG-RC repairs (30 ± 15), and suture-only repairs (42 ± 13) (Figure 7H). Images also showed the linearity of the fibers in that the structure of the enthesis was more amorphous in the suture-only repairs, while the ETG-RC had highly aligned fibers compared to control.

H&E staining was performed for qualitative morphological assessment of the repair. Both repair types demonstrated signs of regeneration as indicated by vascularization and increased cellular density. However, there were distinct differences. H&E staining showed that the enthesis of ETG-RC repair was generally composed of graded zones that resembled native enthesis structure (Figure 7 I-J). This zonal arrangement was not observed in the suture-only repairs, which had less fibrocartilage integration and fewer organized collagen fibers than ETG-RC and

contralateral shoulders. Overall, suture-only repaired shoulders were characterized by an abrupt boundary of scar-like tissue at the tendon-bone interface (Figure 7K).

Significant differences in gross morphology and tissue composition were observed in the instances of tendon mineralization, specifically in suture-only repairs. Representative examples are shown in Figure 8. Image 8A shows that the infraspinatus tendon in animal #1 appears be calcified in the center, which was confirmed by histology. Alizarin Red S staining was performed to visualize the mineralization noted in the radiographs. Alizarin Red S identifies calcium mineralization through the birefringent end-product formed by the Alizarin Red S-calcium complex. Staining of cross-sections taken at the mid-substance of infraspinatus tendons in some suture-only repairs did confirm the presence of calcified mineral, indicating heterotopic ossification in the tendon following rotator cuff repair (Figure 8 B).

Additionally, the morphology of the tendon in animal #2 appears to be abnormally oriented. It lacks uniaxial direction and is twisted (Figure 8 C-E). This may be the result of the ossification at the myotendinous junction, which potentially disrupted fiber alignment and presumably affected force transmission. Due to the rigidity of the tissue, a bone saw was used to cut through the piece shown in image 8E. Such geometrical and morphological changes may ultimately lead to failure of the repair in the future.

Histomorphometric Analysis of the Infraspinatus Muscle

After 6 months of recovery, muscle fiber-type size and percent distribution of fibers containing different myosin heavy (MHC) isoforms were evaluated in the infraspinatus muscle from control, ETG-RC, and suture-only groups. IHC staining was performed with antibodies specific to MHC I (red) and MHC II (green) isoforms (Figure 9A). In the infraspinatus muscle, Type II fibers were most abundant. There were no significant differences in fiber composition of

the ETG-RC and suture-only muscles compared to control (P=0.89 Type II fibers; P=0.89 Type I fibers). In terms of CSA of the type II muscle fibers, no differences were observed compared to contralateral fibers (P=0.25 ETG-RC; P=0.54 suture-only) (Figure 9 B-E).

At the single fiber level, isolated permeabilized muscle fibers were tested for contractile properties. No differences were observed compared to contralateral in fiber CSAs (P=0.90 ETG-RC; P=0.23 suture-only) (Figure 10A), maximum isometric force production (F_o) (P=0.99 ETG-RC; P=0.24 suture-only) (Figure 10B), and specific force (sF_o) (P=0.47 ETG-RC, P=0.501 suture-only) (Figure 10C).

DISCUSSION

The purpose of this study was to evaluate the efficacy of our scaffold-less ETG-RC graft in regenerating the enthesis of the infraspinatus tendon following full-thickness tear in an acute rotator cuff injury in a sheep model. We hypothesized that the utilization of our ETG-RC with traditional double sutures in an infraspinatus tendon repair would improve enthesis regeneration and maintain muscle integrity. The high re-tear rates observed clinically following rotator cuff repair can be partially explained by a lack of enthesis regeneration, as the rotator cuff often ruptures at the tendon-bone insertion site. A technique that successfully regenerates a native enthesis, repairs the mechanical integrity of the tendon to bone insertion, and maintains the structure and function of the muscle will be a significant advancement in the available technologies for repair of massive RC tears.

Various methods are being studied to improve tendon-to-bone healing. These techniques include the application of mechanical reinforcement and/or the introduction of growth factors to the repair site [30]. One common strategy used to improve the functional outcome of rotator cuff repair is mechanical reinforcement of the repair site with a device or scaffold that when used as

an overlay, load-shares the forces across the repaired tendon-to-bone interface, thereby reducing the probability of a tendon re-tear. Many different types of scaffolds have been used in rotator cuff repair, including xenografts, allografts, synthetic grafts, or combinations. Such approaches offer the advantage of mechanical reinforcement during tissue regeneration; however, results are inconsistent and unreliable, likely due to the complex anatomy of the shoulder joint, the variability in the loads placed on the joint during recovery by the activities of individual patients, and the fact that a device used as an overlay does not directly contribute to the regeneration of the enthesis. [31]. Additionally, despite extensive decellularization methods, xenografts and allografts pose an immunogenic risk, leading to the increased interest in alternative technology, such as biodegradable synthetic grafts [32]. A promising and commonly used surgical patch is a degradable patch fabricated from human fascia (biological scaffold) and polylactic-co-glycolic acid (PLGA) and poly-L-lactide (PLLA) materials [31]. Utilization of this patch in an *ex-vivo* canine cadaver model showed that immediately following repair the tendon to bone interface had a higher ultimate load to failure compared to a non-augmented repair. However, an *in vivo* implantation study with a 12-week recovery showed the patch-repaired tendons had a reduced failure load (65%) and lower stiffness (48%) compared to non-augmented controls. While the histological analysis of the repair site demonstrated lack of an immunogenic reaction, a detailed analysis of enthesis regeneration was not performed [33]. Thus, the attribution of proper enthesis regeneration to the mechanism of failure in this *in vivo* study could not be determined. Another commonly used method for patch fabrication is the use of synthetic scaffold materials. One study using gelatin-grafted-PLLA electrospun synthetic patch demonstrated promising functional and biomechanical outcomes in a rat model [34]. Following an 8-week recovery, this study showed significant improvements in fibrocartilage formation and collagen organization at the enthesis.

The repair of RC tears with this synthetic patch resulted in a greater ultimate load-to-failure and stiffness compared to control groups [34]. While these results are encouraging, it should be mentioned that although rats are used in RC tear injury models, rat tissue regeneration is typically accelerated and does not mimic the post-surgical failure rates and scar formation observed in humans and large animal models. In addition, while synthetic materials appear to a biocompatible option for the fabrication of patches used for tendon repair, as they can be fabricated with materials that do not elicit an immune response, there can be cytotoxic effects of the degradation products of such patches. One study found high concentrations of lactic and glycolic acid leeching from a PLLA scaffold impaired osteoblast proliferation [35]. Impairment of osteoblast proliferation has been shown to limit the regeneration of the mineralized fibrocartilage zone comprising a native enthesis. So, while scaffolds offer the mechanical stabilization of the joint during recovery, they do not contribute to the biological aspects of the repair - the regeneration of native tendon and enthesis tissues.

While there has been limited success in the regeneration of the enthesis following RC injury regardless of the method of repair, interventions utilizing growth factors have shown some promise in the promotion of extracellular matrix production, cell proliferation, and cell differentiation which may enhance tissue regeneration and prevent gap formation at the repair site. Rodeo et. al. [36] tested the efficacy of a growth factor cocktail to enhance tendon regeneration and increase the attachment strength of the tendon to the bone in a sheep rotator cuff injury model. They reported that the administration of BMP-2-7, TGF-b-1-3, and FGF growth factors using a type I collagen sponge carrier resulted in improved ultimate load-to-failure after a 12-week recovery time compared to the collagen sponge implant alone or a suture-only repair. However, while the study demonstrated that the growth factor treatment resulted in

increased tissue generation, the resulting tissue was mostly scar tissue rather than native-like tendon regeneration. Thus, when the biomechanical properties were normalized by native-like tendon at the attachment site, the load to failure was not improved compared to the collagen sponge implant or suture-only group [36]. The introduction of multiple growth factors to a repair site during or following repair is promising in that it may improve the initial biomechanical properties of the tendon-bone interface but current interventions are limited by delivery and specificity for stimulating native tendon vs. scar tissue generation.

Thus, our laboratory has designed a tissue-engineered construct, ETG-RC, that does not rely on scaffold or growth factors and shows improved functional outcomes in a sheep model for RC repair. Using our ETG-RC technology in a 6-month recovery model, we demonstrated that the ETG-RC recovered 31% of the modulus of native tendon, and an 11% increase in modulus above a suture-only repair. In addition, histological analysis of the repair site demonstrated positive effects of the ETG-RC technology showing successful zonal regeneration of a native-like enthesis. After 6 months *in vivo*, repair of a torn rotator cuff tendon with an ETG-RC showed a significant increase in collagen alignment at the enthesis compared to suture-only repaired tendons. Previous work in our sheep ACL studies indicate that the constructs are being decellularized during the early stages of remodeling and ultimately may serve as a scaffold for the infiltrating host cells [19-23]. The histological analysis of the tendon-to-bone interface of suture-only repairs was characterized by a layer of poorly organized, cellular, fibrovascular tissue with no evidence of a native-like enthesis. This is significant because the native structural organization of the collagen fibers within the enthesis has been shown to be important in reducing the magnitude of stress concentrations. Any significant deviation from native enthesis anatomy may ultimately result in higher incidence in re-tear at the repair site. Our histology data

showed that ETG-RC repairs showed a regenerated enthesis and not fibrovascular scar tissue. In contrast, suture repairs lacked a transitional region and showed an abrupt divide between tendon and bone with a gap of fibrovascular tissue up to 1.5 mm wide. A previous rotator cuff study has reported gaps up to 18 mm wide [37]. However, it is important to note that our study had a 6-month recovery period, while the above study was only a 3-month recovery [37]. This difference in recovery time may account for the differences in gap length. Additionally, previous work using our technology in five sheep ACL studies indicate that at least a 6-month recovery and up to 2 years is necessary to yield more optimal outcomes [19-23].

In conclusion, our ETG-RC technology resulted in improved healing and regeneration of the four graded zones of a native enthesis. While, the goal of this study was to evaluate enthesis regeneration between the two repair groups, the presence of HO in the tendon of suture-only repairs was an interesting finding. The literature suggests that the HO present in the suture-only group may be the result of an excessive inflammatory response and infiltration of macrophages into the repair site. The literature suggests these macrophages are capable of BMP synthesis which may ultimately lead to increased matrix mineralization at the repair site [38]. Additionally, studies show that balance between macrophage type (M1/M2) is necessary for proper healing and regeneration [39]. Therefore, the absence of HO in the ETG-RC group suggests a difference in the regenerative and inflammatory response between the two repair groups. It is possible that wound healing response in the suture-only repairs was characterized by an imbalance of macrophage type and an overabundance of M2 macrophages, which could lead to excessive fibrosis and matrix deposition [40-41]. Future experiments investigating host cell interactions with the ETG-RC and pathways of inflammation, cellular migration, cytokine expressions, and cellularity will be necessary to determine the mechanism of remodeling toward native tendon.

While the animals in this study did not undergo any rehabilitation treatment, nor were their joints physically immobilized (in stark contrast to human recoveries), we did not observe any changes in muscle structure or function in either group, potentially due to the acute nature of the study. The fact that there are no significant differences in the CSA or force from fibers shows that we did not get the typical muscle atrophy following rotator cuff repair. This was most likely due to the fact that this was not a chronic injury model and the injured site did not exhibit muscle atrophy and tendon retraction as typically observed in the human condition. Thus, future studies will investigate the efficacy of the ETG-RC in a more clinically relevant chronic injury model with rehabilitation.

Acknowledgments: The study was funded by a gift to the Hospital for Special Surgery and University of Michigan department of Orthopaedic Surgery. We would like to acknowledge the technical assistance of Jenna Nutter and Christopher Larkin. Additionally, we would like to acknowledge the University of Michigan Orthopaedic Research Laboratories for their technical assistance.

References

1. American Academy of Orthopaedic Surgeons. 2011. New Guideline on Rotator Cuff

Problems.

2. Lin JC, Weintraub N, Aragaki DR. 2008. Nonsurgical treatment for rotator cuff injury in the elderly. J Am Med Dir Assoc 9:626-632.
3. Lehman C, Cuomo F, Kummer FJ, et al. 1995. The incidence of full thickness rotator cuff tears in a large cadaveric population. Bull Hosp Jt Dis 54:30-31.
4. Derwin KA, Baker AR, Iannotti JP, et al. 2010. Preclinical models for translating regenerative medicine therapies for rotator cuff repair. Tissue Eng Part B Rev 16:21-30.
5. Galatz LM, Ball CM, Teefey SA, et al. 2004. The outcome and repair integrity of completely arthroscopically repaired large and massive rotator cuff tears. J Bone Joint Surg Am 86-A:219-224.
6. Montgomery SR, Petrigliano FA, Gamradt SC. 2012. Failed rotator cuff surgery, evaluation and decision making. Clin Sports Med 31:693-712.
7. Zhang AL, Montgomery SR, Ngo SS, et al. 2014. Arthroscopic versus open shoulder stabilization: current practice patterns in the United States. Arthroscopy 30:436-443.
8. Benjamin M, Kumai T, Milz S, et al. 2002. The skeletal attachment of tendons--tendon "entheses". Comp Biochem Physiol A Mol Integr Physiol 133:931-945.
9. Lu HH, Thomopoulos S. 2013. Functional attachment of soft tissues to bone: development, healing, and tissue engineering. Annu Rev Biomed Eng 15:201-226.
10. Lu HH, Thomopoulos S. 2013. Functional attachment of soft tissues to bone: development, healing, and tissue engineering. Annu Rev Biomed Eng 15:201-226.
11. Waggett AD, Ralphs JR, Kwan AP, et al. 1998. Characterization of collagens and proteoglycans at the insertion of the human Achilles tendon. Matrix Biol 16:457-470.
12. Thomopoulos S, Marquez JP, Weinberger B, et al. 2006. Collagen fiber orientation at the

tendon to bone insertion and its influence on stress concentrations. J Biomech 39:1842-1851.

13. Thomopoulos S, Williams GR, Gimbel JA, et al. 2003. Variation of biomechanical, structural, and compositional properties along the tendon to bone insertion site. J Orthop Res 21:413-419

14. Thomopoulos S, Genin GM, Galatz LM. 2010. The development and morphogenesis of the tendon-to-bone insertion - what development can teach us about healing -. J Musculoskelet Neuronal Interact 10:35-45.

15. Levenda AC, Sanders NR. 2015. A Simplified Approach for Arthroscopic Repair of Rotator Cuff Tear with Dermal Patch Augmentation. Advances in Orthopedic Surgery 2015:7.

16. Barber FA, Herbert MA, Coons DA. 2006. Tendon augmentation grafts: biomechanical failure loads and failure patterns. Arthroscopy 22:534-538.

17. Vunjak-Novakovic G, Altman G, Horan R, et al. 2004. Tissue engineering of ligaments. Annu Rev Biomed Eng 6:131-156.

18. Weitzel PP, Richmond JC, Altman GH, et al. 2002. Future direction of the treatment of ACL ruptures. Orthop Clin North Am 33:653-661.

19. Ma J, Smietana MJ, Kostrominova TY, et al. 2012. Three-dimensional engineered bone-ligament-bone constructs for anterior cruciate ligament replacement. Tissue Eng Part A 18:103-116.

20. Mahalingam VD, Behbahani-Nejad N, Ronan EA, et al. 2015. Fresh versus frozen engineered bone-ligament-bone grafts for sheep anterior cruciate ligament repair. Tissue Eng Part C Methods 21:548-556.

21. Mahalingam VD, Behbahani-Nejad N, Horine SV, et al. 2015. Allogeneic versus autologous derived cell sources for use in engineered bone-ligament-bone grafts in sheep anterior cruciate ligament repair. Tissue Eng Part A 21:1047-1054.

22. Florida SE, VanDusen KW, Mahalingam VD, et al. 2016. In vivo structural and cellular remodeling of engineered bone-ligament-bone constructs used for anterior cruciate ligament reconstruction in sheep. Connect Tissue Res 57:526-538.

23. Mahalingam V, Wojtys EM, Wellik DM, et al. 2016. Fresh and Frozen Tissue-Engineered Three-Dimensional Bone-Ligament-Bone Constructs for Sheep Anterior Cruciate Ligament Repair Following a 2-Year Implantation. Biores Open Access 5:289-298.

24. National Research Council. Guide for the Care and Use of Laboratory Animals, Eighth Edition. Washington, DC : The National Academies Press, 2011.

25. Mendias CL, Kayupov E, Bradley JR, et al. 2011. Decreased specific force and power production of muscle fibers from myostatin-deficient mice are associated with a suppression of protein degradation. J Appl Physiol (1985) 111:185-191.

26. Panchangam A, Claflin DR, Palmer ML, et al. 2008. Magnitude of sarcomere extension correlates with initial sarcomere length during lengthening of activated single fibers from soleus muscle of rats. Biophys J 95:1890-1901.

27. Claflin DR, Larkin LM, Cederna PS, et al. 2011. Effects of high- and low-velocity resistance training on the contractile properties of skeletal muscle fibers from young and older humans. J Appl Physiol (1985) 111:1021-1030.2.

28. Gumucio JP, Davis ME, Bradley JR, et al. 2012. Rotator cuff tear reduces muscle fiber specific force production and induces macrophage accumulation and autophagy. J Orthop

Res 30:1963-1970.

29. Cohen DB, Kawamura S, Ehteshami JR, et al. 2006. Indomethacin and celecoxib impair rotator cuff tendon-to-bone healing. Am J Sports Med 34:362-369.

30. Ratcliffe A, Butler DL, Dyment NA, et al. 2015. Scaffolds for tendon and ligament repair and regeneration. Ann Biomed Eng 43:819-831.

31. Thangarajah T, Pendegrass CJ, Shahbazi S, et al. 2015. Augmentation of Rotator Cuff Repair With Soft Tissue Scaffolds. Orthop J Sports Med 3:2325967115587495.

32. Qazi TH, Mooney DJ, Pumberger M, et al. 2015. Biomaterials based strategies for skeletal muscle tissue engineering: existing technologies and future trends. Biomaterials 53:502-521.

33. Baker AR, McCarron JA, Tan CD, et al. 2012. Does augmentation with a reinforced fascia patch improve rotator cuff repair outcomes? Clin Orthop Relat Res 470:2513-2521.4.

34. Zhao S, Xie X, Pan G, et al. 2015. Healing improvement after rotator cuff repair using gelatin-grafted poly(L-lactide) electrospun fibrous membranes. J Surg Res 193:33-42.

35. Meyer F, Wardale J, Best S, et al. 2012. Effects of lactic acid and glycolic acid on human osteoblasts: a way to understand PLGA involvement in PLGA/calcium phosphate composite failure. J Orthop Res 30:864-871.

36. Rodeo SA, Potter HG, Kawamura S, et al. 2007. Biologic augmentation of rotator cuff tendon-healing with use of a mixture of osteoinductive growth factors. J Bone Joint Surg Am 89:2485-2497.

37. Kovacevic D, Rodeo SA. 2008. Biological augmentation of rotator cuff tendon repair. Clin Orthop Relat Res 466:622-633.

38. O'Brien EJ, Frank CB, Shrive NG, et al. 2012. Heterotopic mineralization (ossification or

calcification) in tendinopathy or following surgical tendon trauma. Int J Exp Pathol 93:319-331.

39. Schlundt C, El Khassawna T, Serra A, et al. 2015. Macrophages in bone fracture healing: Their essential role in endochondral ossification. Bone.

40. Meneghin A, Hogaboam CM. 2007. Infectious disease, the innate immune response, and fibrosis. J Clin Invest 117:530-538.

41. Eaton KV, Yang HL, Giachelli CM, et al. 2015. Engineering macrophages to control the inflammatory response and angiogenesis. Exp Cell Res 339:300-309.

FIGURE LEGENDS

Figure 1. Fabrication process of ETG-RCs and histological characterization. (A) Bone marrow stromal cells isolated from a bone marrow aspiration were obtained from a male donor sheep and were cultured in vitro using previously described protocols [20-21]. After reaching confluence, the monolayer spontaneously delaminated around constraint pins, forming a 3D cylindrical construct. Six of these single tendon constructs were then placed side-by-side and allowed to fuse. At the opposite end, the six constructs were split into three prongs. The ETG-RC was fully formed after 7 weeks in culture. (B) H&E stained cross-section of ETG-RC at 7 weeks *in vitro* and imaged at 20x magnification. (C) Picrosirius red stained cross-section of ETG-RC at 7 weeks *in vitro* and imaged at 10x magnification. (D) Longitudinal section of Picrosirius red stained ETG-RC after 7 weeks *in vitro* and imaged at 10X magnification under brightfield to show collagen content. (E) Longitudinal section of Picrosirius red stained ETG-RC after 7 weeks *in vitro* and imaged at 10X magnification. Image visualized under polarized light to show collagen alignment. (F) Longitudinal section of ETG-RC after 7 weeks *in vitro.* Immunohistochemical

staining for Elastin showed positive staining. Image taken at 20x magnification with scale bar indication 200 μm.

Figure 2. A pictorial representation of the ETG-RC surgical implantation. (A) In vitro ETG-RC, approximately 6cm in length. (B) Tendon fixation end of ETG-RC passed through infraspinatus tendon. (C) Bone-fixation end of ETG-RC passed through a drilled humeral bone tunnel. Drilled bone tunnel outlined in blue. (D) Completed double row suture repair with ETG-RC inserted. (E) Completed double row suture-only repair.

Figure 3. Custom-made grip design with humerus and scapula mounted uniaxially to the MTS. Arrow points to infraspinatus tendon.

Figure 4. Radiography and gross morphology of the enthesis at 6 months. (A-C) Radiographs of representative shoulders from each group. Arrows point to anchor screws and site of repair. (D-F) Gross view of representative infraspinatus tendons from each group on day of necropsy.

Figure 5. Infraspinatus tendon mineralization. (A) Control of ETG-RC repair. (B) ETG-RC repair. (C) Control of suture-only repair. Arrow points to region of mineralization (D) Suture-only repair. (E) Difference in grayscale values of ETG-RC and suture-only repairs, normalized to contralateral shoulders. (#) Denotes significance $P<0.05$ compared to ETG-RC. Values are reported as mean ± SD (n=8 from ETG-RC and n=11 from suture-only).

Figure 6. Rotator Cuff Stiffness. (*) Denotes significance $P < 0.05$ compared to control shoulder. Error bars represent ± SD.

Figure 7. Collagen Alignment, Fibrocartilage Formation, and H&E at Enthesis. (A-C) Representative images of picrosirius red staining. Images visualized under polarized light and imaged at 4X magnification. (A) Control shoulder, (B) ETG-RC repair, (C) Suture-only repair. (D) Mean grayscale values. (#) Denotes statistical significance compared to control shoulder ($p < 0.05$). (*) Denotes statistical significance compared to ETG shoulder. Error bars represent ± SD. (E-G) Fibrocartilage Formation at Enthesis. Images were taken at 4X magnification. (E) Control shoulder, (F) ETG-RC repair, (G) Suture-only repair. (H) Percent of metachromasia at the enthesis. (I-K) Representative images of H&E. Images were taken at 20x magnification. (I) Control shoulder, (J) ETG-RC repair, (K) Suture-only repair. Arrows points to tendon-bone interface outlined in yellow.

Figure 8. Mineralization in Suture-only Repair. (A) Gross view of infraspinatus tendon in Animal #1. Arrow points to calcified center. (B) Alizarin stained cross-section of infraspinatus tendon of Animal # 1 shows presence of mineralization. Arrow points to calcified center. Image visualized under polarized light and imaged at 4X magnification. (C) Gross view of infraspinatus tendon in Animal # 2. Tendon lacks uniaxial direction and is twisted. (D) Cross-sectional view of infraspinatus tendon in Animal #2. Arrow points to calcified center. (E) Gross view of myotendinous junction in Animal # 2. Arrow points to ossification of myotendinous junction.

Figure 9. Muscle fiber type size and percentage of composition. (A) Representative images indicating different fiber types of control, ETG-RC, suture-only repairs, respectively (B) Cross-sectional area (CSA) of slow-twitch fibers (C) CSA of fast-twitch fibers (D) percentage of distribution of slow-twitch fibers from control, ETG-RC, and suture-only infraspinatus muscles. (E) Percentage of distribution of fast-twitch fibers from control, ETG-RC, and suture-only infraspinatus muscles. Values are reported as mean ± SD (n=9 muscles from controls and n=5 from repair groups).

Figure 10. Fiber contractility. (A) Fiber cross-sectional area (CSA), (B) maximum isometric force (Fo), and (C) specific force (sFo) of control and repaired infraspinatus muscles. Values are reported as mean ± SD (n=6 muscles from controls and n=3 from repair groups).

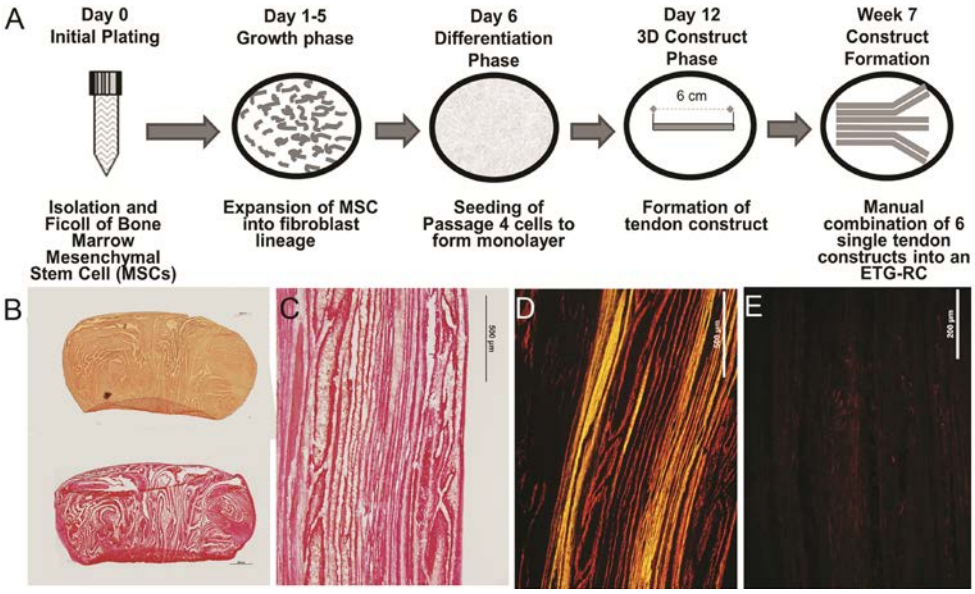

Figure 1

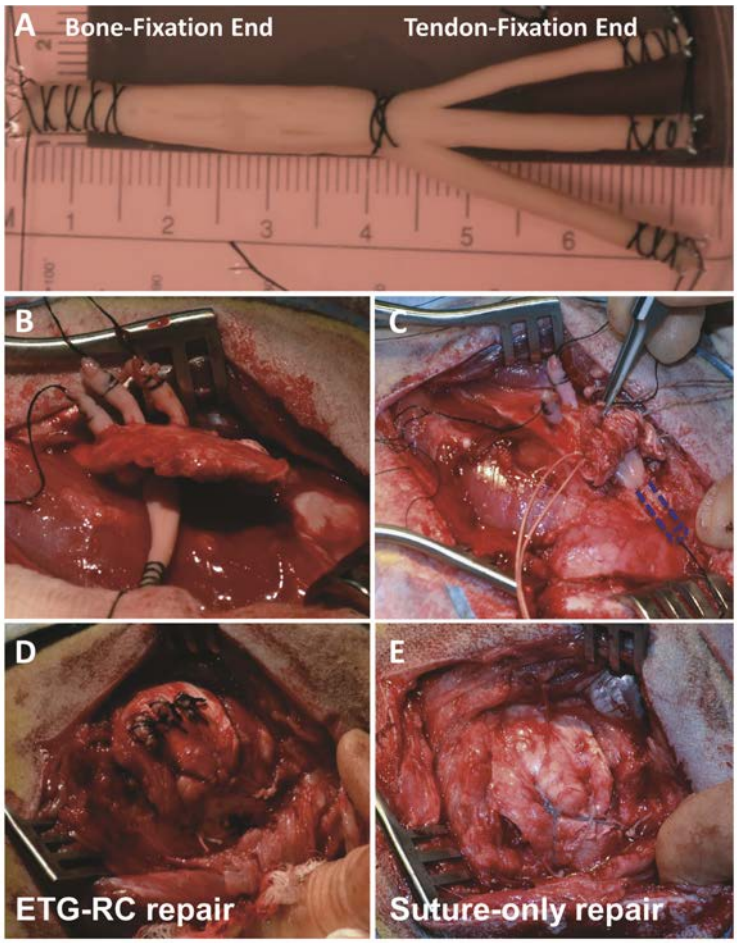

Figure 2

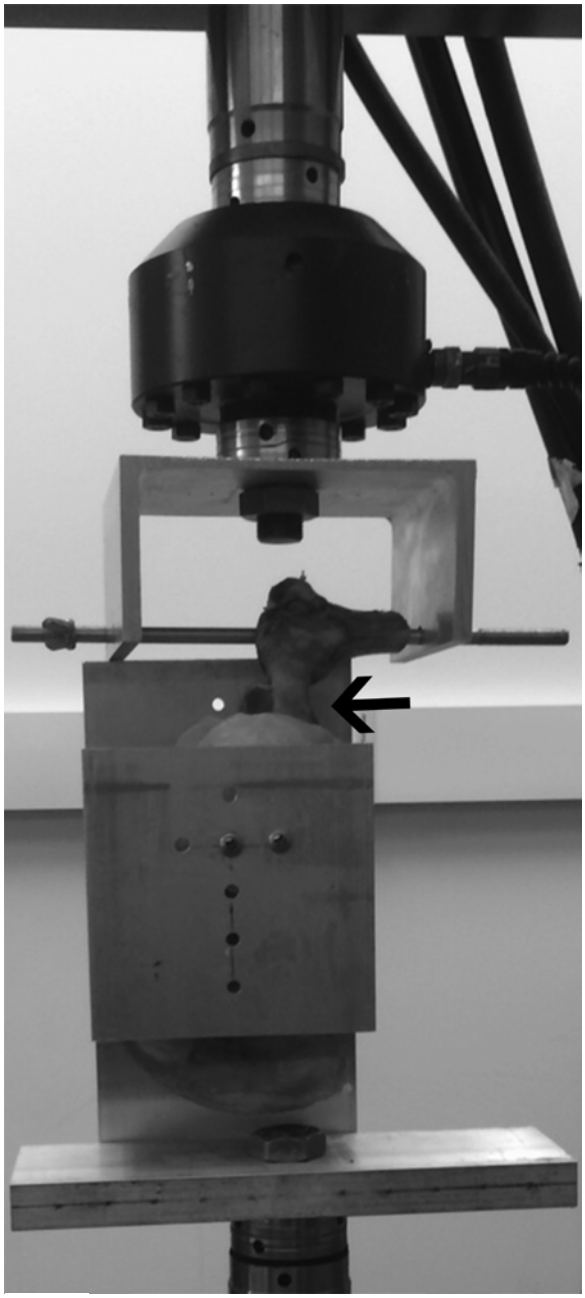

Figure 3

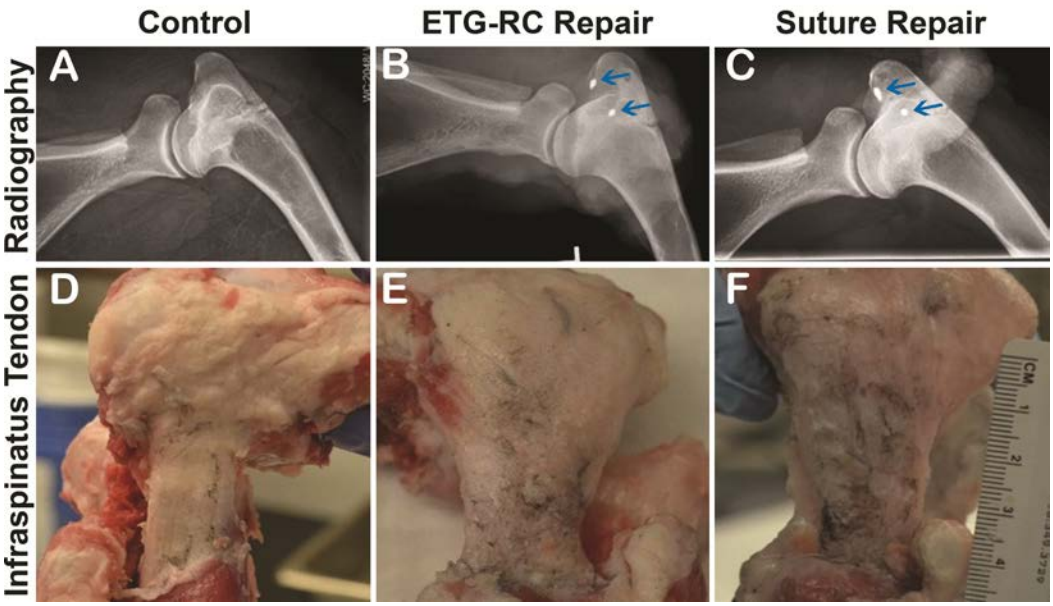

Figure 4

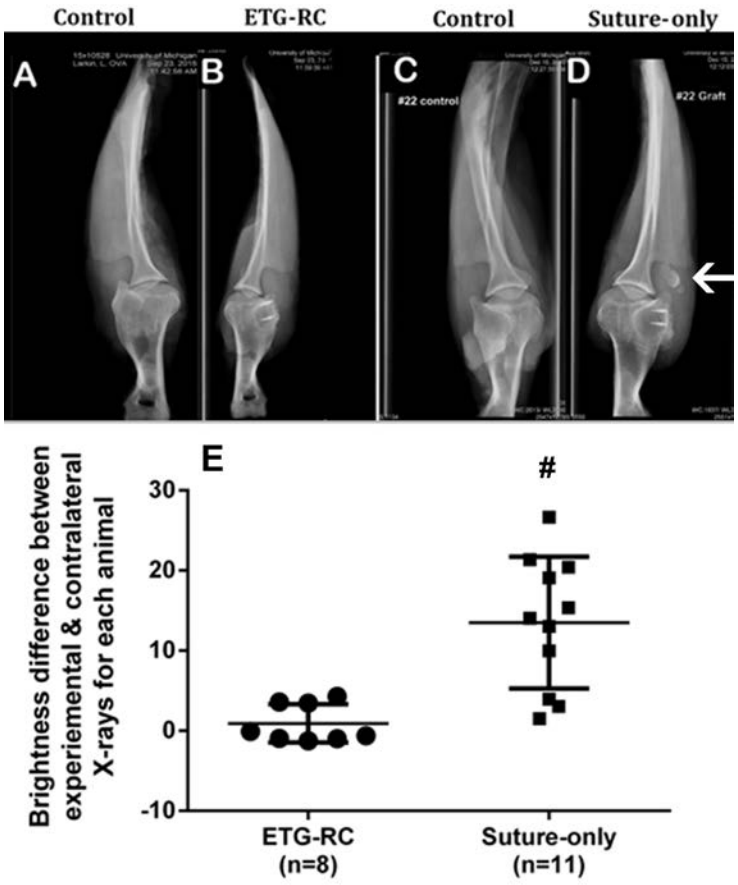

Figure 5

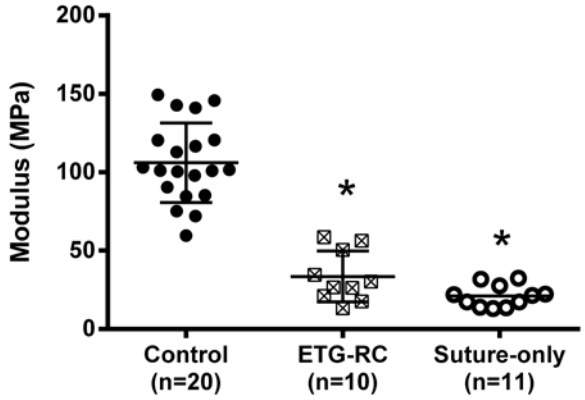

Figure 6

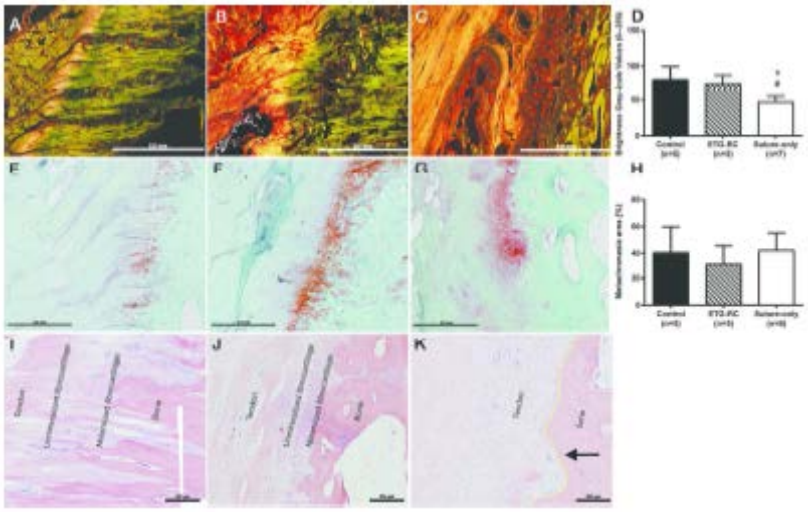

Figure 7

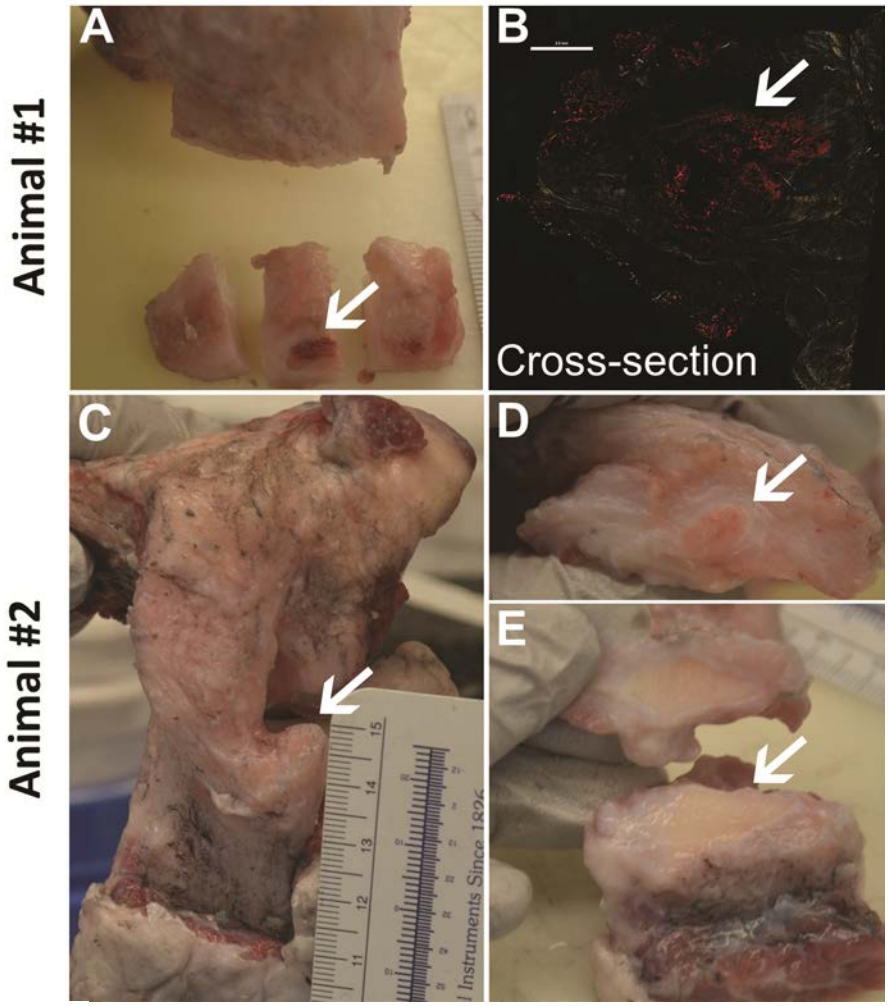

Figure 8

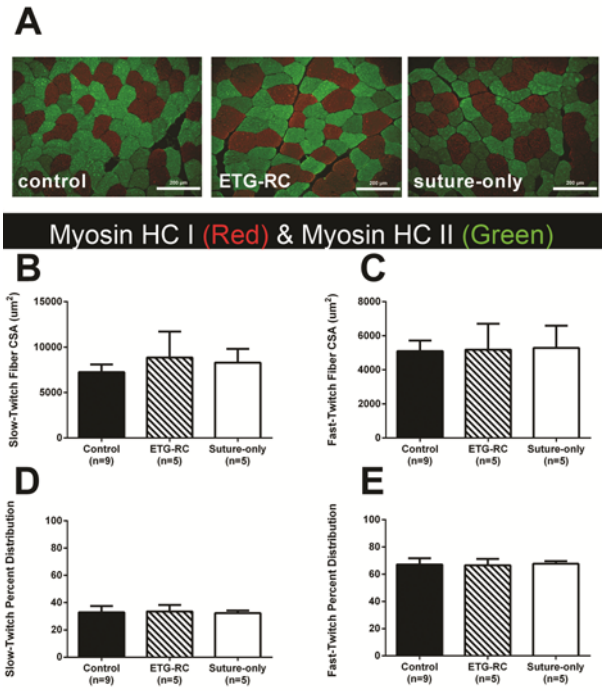

Figure 9

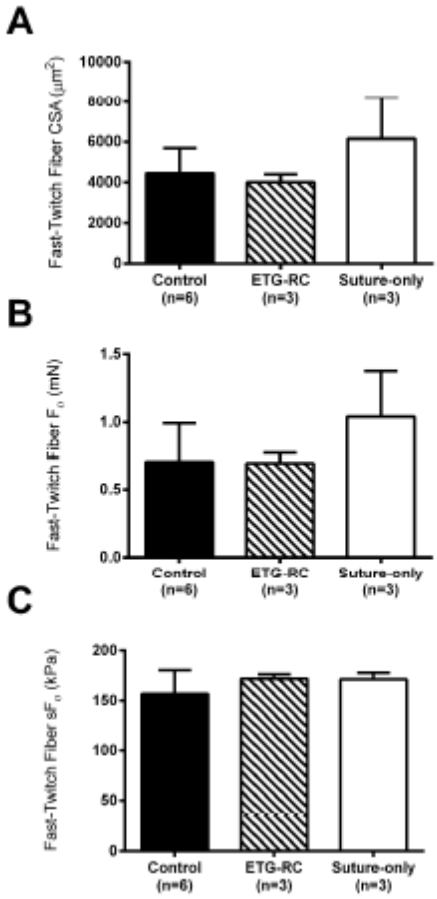

Figure 10